Optimal Distributed Control of a Flexible Spacecraft During a Large-Angle Maneuver

James D. Turner* and Hon M. Chun†
The Charles Stark Draper Laboratory, Cambridge, Massachusetts

This paper discusses the solution of the necessary conditions obtained from Pontryagin's principle, for the problem of optimal large-angle single-axis maneuvers of a flexible spacecraft possessing a distributed control system. A single-stage continuation method is presented for the solution of the resulting two-point boundary-value problem. Starting iteratives for the initial costate variables are obtained by neglecting the kinematic nonlinearity in the state equation which leads to a closed form solution algorithm. The continuation process then increases the participation of the kinematic nonlinearity in a sequence of neighboring optimal solutions (in essence a method of successive linearizations), converging finally to the nonlinear problem of interest.

I. Introduction

A PROBLEM of current interest is the rotational and configuration control of flexible spacecraft. This paper considers the problem of optimal large-angle single-axis maneuvers with simultaneous vibration suppression when a distributed control system is employed. The control system being considered is distributed in the sense that control is applied at several either rigid or flexible points on the vehicle's structure.

The problem of large-angle maneuvers for both rigid and flexible spacecraft has recently been treated by a number of investigators. In the case of rigid vehicles, Junkins and Turner[1] presented the nonsingular necessary conditions for large-angle three-dimensional maneuvers of asymmetric vehicles. They obtained a nonlinear solution by introducing a boundary condition continuation or homotopy method, which reliably solves the resulting two-point boundary-value problem (TPBVP). When flexible vehicles restricted to single-axis maneuvers are considered, a number of investigators working independently have obtained essentially equivalent results for the time-invariant case. For example, Swigert[2] assumed a specialized Fourier series for the unknown control torque, where the coefficients in the series are determined by requiring that the following two conditions be satisfied: first, that the integral of the square of the control torque be minimized; and second, that the maneuver satisfy the prescribed terminal boundary conditions for the problem. Markley[3] considered the effects of selecting different performance indices for the problem of controlling a flexible body modeled with a single flexible mode. Breakwell[4] addressed the problem of controlling several flexible modes, presented results for a feedback control system, and reported experimental verification of the resulting control law formulation. Alfriend et al.[5] considered a frequency response interpretation of optimal slewing maneuvers. Turner and Junkins[6] presented results for controlling several flexible modes for both linear and nonlinear formulations of the equations of motion. In particular, they introduced a differential equation continuation or homotopy method for reliably solving the resulting nonlinear TPBVP. As a further development of Refs. 1 and 6, the authors present herein the necessary extensions when a distributed control system is employed in the flexible body case.

The specific model considered (Fig. 1) consists of a rigid hub with four identical elastic appendages attached symmetrically about the central hub. Only the case of a single-axis maneuver with the flexible members restricted to displacements in the plane normal to the axis of rotation is considered. Furthermore, it is assumed that the body (as a whole) experiences only antisymmetric deformation modes (Fig. 2). The control system for the vehicle is taken to consist of a single controller in the rigid part of the structure and four appendage controllers, one assumed to be located half-way along the span of each of the four appendages. The extension to the case of multiple controllers along each appendage is straightforward; however, only the single appendage controller case is presented in this paper.

The necessary conditions for the optimal single-axis maneuver are presented in two parts. The first part (Secs. II-IV) consists of the formulation and solution of the linearized equations. The second part (Sec. V) consists of the presentation of the nonlinear equations where the nonlinearity is both kinematic and structural in nature. In Sec. VI a differential equation continuation method is presented for solving the nonlinear TPBVP, which makes efficient use of

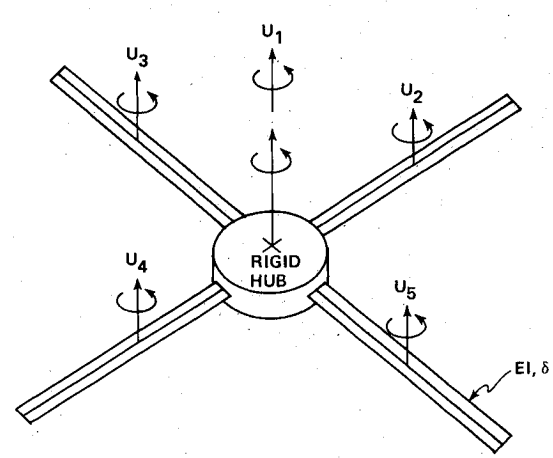

Fig. 1 Undeformed structure.

Presented at the 3rd VPI&SU/AIAA Symposium on Dynamics and Control of Large Flexible Spacecraft, Blacksburg, Va., June 15-17, 1981; submitted Sept. 13, 1982; revision received May 12, 1983.

*Dynamics Section Chief, Advanced Systems Department. Member AIAA.
†Member of Technical Staff, Advanced Systems Department. Member AIAA.

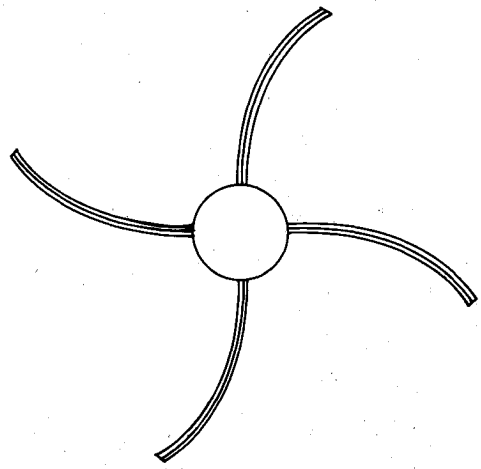

Fig. 2 Antisymmetric deformation.

the initial costates determined in Sec. IV. Section VII presents the case where the final angle is to be determined by the optimal control problem. In Sec. VIII we provide numerical results which support the validity and utility of the formulations described herein.

II. Equations of Motion

For the vehicle being considered, the equations of motion can be obtained from Hamilton's extended principle.[7]

$$\int_{t_1}^{t_2} (\delta\ell + \delta w)\,dt = 0 \quad \text{subject to} \quad \delta\theta = \delta u = 0 \quad \text{at} \quad t_1, t_2 \tag{1}$$

where $\ell = T - V$ is the system Lagrangian, δw represents the virtual work, $\delta\theta$ represents a virtual rotation, and δu represents a virtual elastic displacement.

The kinetic and potential energy expressions for the vehicle can be shown to be

$$T = \frac{1}{2}\dot{\theta}^2\left[\hat{I} + 4\int_r^{r+L}(u^2 - P^2)\,dm\right] + 2\int_r^{r+L}\dot{u}^2\,dm + 4\dot{\theta}\int_r^{r+L} x\dot{u}\,dm \tag{2}$$

$$V = 2\int_r^{r+L} EI\left[\frac{\partial^2 u}{\partial x^2}\right]^2 dx, \tag{3}$$

where

$$P^2 = \frac{1}{2}\left[(r+L)^2 - r^2 - x^2\right]\left[\frac{\partial u}{\partial x}\right]^2$$

and $\hat{I}$ denotes the moment of inertia of the undeformed vehicle about the axis of rotation, r denotes the radius of the rigid hub, L denotes the undeformed length of the elastic appendages, x is the distance from the center of the rigid hub, P^2 denotes a first order correction for arc length along an appendage, and EI denotes the flexural rigidity of each of the appendages.

The virtual work in this example can be shown to be

$$\delta w = \sum_{k=1}^{n^*} Q_k \delta q_k \quad (n^* = \text{number of generalized coordinates}) \tag{4}$$

where Q_k denotes the kth generalized force and q_k denotes the kth generalized coordinate. Before applying Hamilton's extended principle, we express (by the assumed modes method[8]) the elastic displacements as the following series:

$$u = \sum_{k=1}^{n} \eta_k(t)\,\phi_k(x-r) \tag{5}$$

where $\eta_k(t)$ represents the kth time-varying amplitude, $\phi_k(x-r)$ represents the kth assumed admissible mode shape (in this instance a comparison function), and n represents the number of terms used in the approximation.

On introducing Eq. (5) into Eqs. (2) and (3), we obtain for the system Lagrangian

$$\ell = \frac{\hat{I}}{2}\dot{\theta}^2 + \frac{1}{2}\dot{\eta}^T M_{\eta\eta}\dot{\eta} + \dot{\theta}\dot{\eta}^T M_{\theta\eta} - \frac{1}{2}\dot{\theta}^2\eta^T[\mathfrak{M} - M_{\eta\eta}]\eta - \frac{1}{2}\eta^T K_{\eta\eta}\eta \tag{6}$$

where

$$\eta = [\eta_1, \eta_2, \ldots, \eta_n]^T, \quad (\,)' \equiv \frac{d}{dx}(\,), \quad (\,)'' \equiv \frac{d^2}{dx^2}(\,)$$

$$[M_{\eta\eta}]_{kp} = 4\int_r^{r+L} \phi_k(x-r)\,\phi_p(x-r)\,dm \qquad (n\times n)$$

$$[M_{\theta\eta}]_k = 4\int_r^{r+L} x\phi_k(x-r)\,dm \qquad (n\times 1)$$

$$[\mathfrak{M}]_{kp} = 4\int_r^{r+L} \frac{1}{2}\left[(r+L)^2 - r^2 - x^2\right] \times \phi_k'(x-r)\,\phi_p'(x-r)\,dm \qquad (n\times n)$$

$$[K_{\eta\eta}]_{kp} = 4\int_r^{r+L} EI\phi_k''(x-r)\,\phi_p''(x-r)\,dx \qquad (n\times n)$$

As shown in Ref. 9 we find for Q_k

$$Q_1 = u_1 + 4u_2 \qquad \text{(rigid body torque)} \tag{7}$$

$$Q_k = 4\phi_{k-1}'(x_p - r)\,u_2 \qquad \text{(elastic appendage torque)} \quad (k = 2,3,\ldots,n) \tag{8}$$

where x_p is the coordinate locating the point of application of the control torque on the elastic appendage, u_1 is the torque applied to the rigid body, and u_2 is the torque applied to each of the four elastic appendages. Equation (8) is obtained in the following way: first, the control torque acting on an elastic appendage is replaced by an equivalent couple; and second, a limiting process is carried out which leads directly to Eq. (8).

Substituting Eqs. (6-8) into Eq. (1) yields Lagrange's equations

$$\frac{d}{dt}\left[\frac{\partial\ell}{\partial\dot{\theta}}\right] - \frac{\partial\ell}{\partial\theta} = u_1 + 4u_2 \tag{9}$$

$$\frac{d}{dt}\left[\frac{\partial\ell}{\partial\dot{\eta}}\right] - \frac{\partial\ell}{\partial\eta} = Fu_2 \tag{10}$$

where

$$F = 4[\phi_1'(x_p - r)\,\phi_2'(x_p - r)\ldots\phi_n'(x_p - r)]^T$$

From which the equations of motion follow as

$$(\hat{I} - \eta^T M^*\eta)\ddot{\theta} + M_{\theta\eta}^T\ddot{\eta} - 2\dot{\theta}\dot{\eta}^T M^*\eta = u_1 + 4u_2 \tag{11}$$

$$M_{\theta\eta}\ddot{\theta} + M_{\eta\eta}\ddot{\eta} + [K_{\eta\eta} + \dot{\theta}^2 M^*]\eta = Fu_2 \tag{12}$$

where

$$M^* = \mathfrak{M} - M_{\eta\eta}$$

III. State Space Formulation

The state space form of Eqs. (11) and (12) is obtained by making a small deflection assumption which permits the quadratic deflection terms in Eq. (11) to be dropped, leading to

$$M\ddot{\zeta} + K\zeta = Pu - \alpha\dot{\theta}^2 R\zeta \tag{13}$$

where

$$\zeta = \begin{Bmatrix} \theta \\ \eta \end{Bmatrix}, \quad M = \begin{bmatrix} \hat{I} & M_{\theta\eta}^T \\ M_{\theta\eta} & M_{\eta\eta} \end{bmatrix}, \quad K = \begin{bmatrix} 0 & \mathbf{0}^T \\ \mathbf{0} & K_{\eta\eta} \end{bmatrix}$$

$$P = \begin{bmatrix} 1 & 4 \\ \mathbf{0} & F \end{bmatrix} \quad R = \begin{bmatrix} 0 & \mathbf{0}^T \\ \mathbf{0} & M^* \end{bmatrix} \quad u = [u_1 u_2]^T$$

and $M = M^T$ (positive definite), $K = K^T$ (positive semi-definite), and α is the continuation parameter.

Introducing the coordinate transformation

$$\zeta = Et \tag{14}$$

where E is the matrix of normalized eigenvectors for the generalized eigenvalue problem for M and K such that

$$E^T M E = I \quad \text{and} \quad E^T K E = \Delta \tag{15}$$

the equation of motion becomes

$$\ddot{t} + \Delta t = Vu - \alpha(v^T\dot{t})^2 Lt, \qquad V = E^T P, \qquad L = E^T R E \tag{16}$$

Defining the state variable subsets

$$s_1 = t \qquad s_2 = \dot{t} \tag{17}$$

and letting $s = [s_1^T s_2^T]^T$, the state space equation becomes

$$\dot{s} = A(s,\alpha)s + Bu \tag{18}$$

where

$$A(s,\alpha) = \begin{bmatrix} 0 & I \\ A_{21}(s,\alpha) & \mathbf{0} \end{bmatrix}, \quad A_{21}(s,\alpha) = -\Delta - \alpha(v^T s_2)^2 L$$

$$v = E^T[10^T]^T = [E_{11}E_{12}\ldots E_{1N}]^T, \quad B = \begin{Bmatrix} \mathbf{0} \\ V \end{Bmatrix} \qquad (N = n+1)$$

IV. Optimal Control Problem

A. Statement of Problem

The optimal control problem involves the rotational dynamics of a flexible space vehicle restricted to a single-axis large-angle maneuver, where the system dynamics are governed by Eq. (18). In particular, the problem is to seek a solution of Eq. (18) satisfying the prescribed terminal states $\zeta_0, \dot{\zeta}_0, \zeta_f, \dot{\zeta}_f$, where $\eta_f = \dot{\eta}_f = \mathbf{0}$, and which minimizes the performance index

$$J = \frac{1}{2}\int_{t_0}^{t_f} [u^T W_{uu} u + s^T W_{ss} s]\,dt \tag{19}$$

Although the particular choice of weighting matrices W_{ss} and W_{uu} significantly affects the computational effort and resulting maneuvers, the scheme used for determining W_{ss} and W_{uu} is not discussed in this paper. For more details see Ref. 9.

B. Derivation of Necessary Conditions from Pontragin's Principle

In preparing to make use of Pontryagin's necessary conditions, the Hamiltonian functional is formed as

$$H = \tfrac{1}{2}(u^T W_{uu} u + s^T W_{ss} s) + \lambda^T(A(s,\alpha)s + Bu) \tag{20}$$

Setting α to zero in Eq. (20) for the linear solution, the state, costate, and control necessary conditions are obtained as follows.

State equation

$$\dot{s} = As - BW_{uu}^{-1}B^T\lambda \tag{21}$$

Costate equation

$$\dot{\lambda} = -W_{ss}s - A^T\lambda \tag{22}$$

Control equation

$$u = -W_{uu}^{-1}B^T\lambda \tag{23}$$

C. Solution for the Initial Costates

The unknown initial costate defining the solution for Eqs. (21) and (22) is obtained from the following equation[1,6,9]:

$$\lambda(0) = \phi_{s\lambda}^{-1}\{s(t_f) - \phi_{ss}s(0)\} \tag{24}$$

where $\phi_{s\lambda}$ and ϕ_{ss} are partitions of the exponential matrix[10,11]

$$e^{\Omega(t_f - t_0)} = \begin{bmatrix} \phi_{ss} & \phi_{s\lambda} \\ \phi_{\lambda s} & \phi_{\lambda\lambda} \end{bmatrix} \tag{25}$$

where

$$\Omega = \begin{bmatrix} A & -BW_{uu}^{-1}B^T \\ -W_{ss} & -A^T \end{bmatrix} \begin{matrix} \text{constant} \\ = \text{coefficient matrix} \end{matrix}$$

The following two sections involve the solution of a problem of the same structure, but including the previously neglected kinematic nonlinearity. The idea is to use the solution to Eq. (24) as starting iteratives for a continuation or homotopy chain method, which will solve this related nonlinear problem.

V. Optimal Control Problem Including Kinematic Nonlinearities

Due to the similarity in structure with the presentation in Sec. IV, only key equations are given. Defining the optimal control problem as in Sec. IV.A leads to state, costate, and control necessary conditions which are summarized as:

State equation

$$\dot{s} = A(s,\alpha)s - BW_{uu}^{-1}B^T\lambda \tag{26}$$

Costate equation

$$\dot{\lambda} = -W_{ss}s - C(s,\alpha)\lambda \tag{27}$$

Control equation

$$u = -W_{uu}^{-1}B^T\lambda \tag{28}$$

where

$$C(s,\alpha) = \begin{bmatrix} \mathbf{0} & A_{21}^T(s,\alpha) \\ I & -2\alpha(v^T s_2)vs_1^T L^T \end{bmatrix}$$

VI. Continuation Method for the Solution of the Nonlinear TPBVP

The motivation for introducing the parameter α in Eq. (13) comes about from a simple observation. That is, if it is very difficult to obtain a solution for the operator equation

$$f(x)=0 \tag{29}$$

directly, then the numerical solution of Eq. (29) can frequently be directly obtained by solving the family of problems

$$F(x,\alpha)=0 \tag{30}$$

where α is a parameter which varies from 0 to 1.

The family $F(x,\alpha)$ is chosen so that 1) $F(x,1)\equiv f(x)$, 2) x_0 is an easily calculated (unique) solution of $F(x,0)=0$, and 3) $F(x,\alpha)$ is a continuous function of α. The solution process proceeds as follows. The sequence of parameter values $\{0=\alpha_0<\alpha_1<\alpha_2<\cdots<\alpha_p=1\}$ is chosen where the value of α_p is either preset or determined during the iterative process using the techniques discussed in Schmidt[12] and Deuflhard et al.[13] The solution x_{i+1} of

$$F(x,\alpha_{i+1})=0 \tag{31}$$

is obtained using an iterative method since F is in general nonlinear (in particular, the iterative quasi-Newton method used in this paper is described in Dennis and Schnabel,[14] Greenstadt,[15] and Goldfarb.[16]) As starting estimates for x_{i+1}, one could use either the converged value of x_i, or an extrapolated value for x_{i+1} based on the behavior of the converged x_i for back α values. Based on the authors' own numerical experiments, it has been found that using the second method above accelerates convergence in the solution for x_{i+1}, and the method works both efficiently and reliably.

On making the identification for F in Eqs. (26), (27), and (31), one obtains

$$F(s,\lambda,\alpha)=\begin{Bmatrix} \dot{s}-A(s,\alpha)s+BW_{uu}^{-1}B^T\lambda \\ \dot{\lambda}+W_{ss}s+C(s,\alpha)\lambda \\ s_f-s(s(0),\lambda(0),t_f) \end{Bmatrix}=\begin{bmatrix} 0 \\ 0 \\ 0 \end{bmatrix} \tag{32}$$

In addition, recalling that $s(0)$ is given and $\lambda(0)$ is provided by Eq. (24) for $\alpha=0$, one finds that in Eq. (32), the operator equation to be satisfied consists of the state and costate differential equations, as well as terminal constraints on the final values of the state. These observations thus motivate the following successive approximation strategy for solving the nonlinear TPBVP, for homotopy chain parameters α_k $(k=1,\ldots,p)$.

Letting the approximate initial costates be denoted by

$$\lambda_0=\lambda(t_0) \tag{33}$$

the differential correction strategy is to seek the correction vector $\Delta\lambda$ subject to the terminal constraint

$$s_f-s(\lambda_0+\Delta\lambda,t_f)=0 \tag{34}$$

where s_f denotes the vector of desired terminal boundary conditions for the variable s.

On linearizing Eq. (34), we obtain

$$s_f-s-A_{s\lambda}\Delta\lambda=0 \tag{35}$$

where s denotes the numerically integrated solution of Eq. (26), using as initial conditions $s(t_0)$ and the approximate costate λ_0, and

$$A_{s\lambda}=\left[\begin{array}{c|c} \dfrac{\partial s^T}{\partial\lambda_0} & t_f \end{array}\right]^T=\phi_{s\lambda} \tag{36}$$

where $\phi_{s\lambda}$ denotes the block of the state transition matrix for the variables s and λ. Next, defining

$$\Delta s_f=s_f-s \tag{37}$$

and introducing Eq. (37) into Eq. (35) yields

$$\Delta s_f=\phi_{s\lambda}\Delta\lambda \tag{38}$$

The solution for Eq. (38) is easily obtained by using a standard linear equation solver. The calculation of the required partial derivatives for the nonlinear problem is dealt with in Ref. 9.

The previous discussion can be summarized as the differential correction algorithm in Fig. 3 for refining the given approximate initial costates λ_0; by these means, a precise solution for the TPBVP can be obtained (provided the starting estimates are "sufficiently good").

The only significant assumption en route to the algorithm is the local linearization of Eq. (34) to obtain Eq. (35). The only open question remaining about the algorithm is: How to choose the sequence of α values? Clearly, this process could be made adaptive; however, in the example maneuvers presented in Sec. VIII the following preset sequence has proven successful

$$\{\alpha_0,\alpha_1,\ldots,\alpha_3\}=\{0.0,0.05,0.5,1.0\} \tag{39}$$

Using the sequence of α values given in Eq. (39), the algorithm in Fig. 3 is used with converged costate extrapolations as starting estimates.

VII. Linear Slewing Maneuver with Free Final Angles

This section deals with the linear optimal control for slewing maneuvers in which the final angular rate, rather than the final angle, is important.

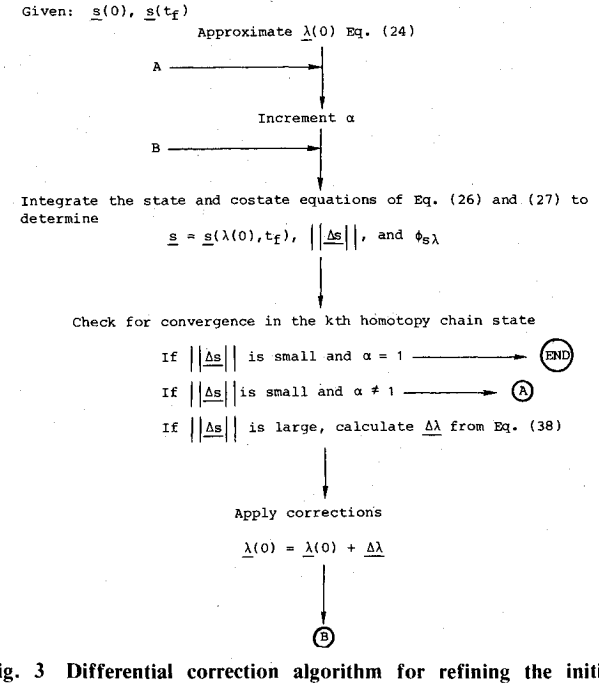

Fig. 3 Differential correction algorithm for refining the initial costates.

A. Transformation Between Modal Space and Physical Space

Since the free final angle transversality condition is naturally defined in terms of physical rather than modal coordinates, the following two transformation equations permit the use of the results of Sec. IV. First the modal space state transition matrix $\phi(t_f,t_0)$ of Eq. (25) is mapped to physical space via the transformation:

$$\Phi(t,t_0)=\Theta\phi(t,t_0)\Theta^{-1} \tag{40}$$

where

$$\Theta=E\otimes E\otimes ME\otimes ME$$

$$\Theta^{-1}=E^TM\otimes E^TM\otimes E^T\otimes E^T$$

where $\otimes$ denotes the direct sum.

Second, once the physical space initial conditions have been obtained, the modal space initial conditions are obtained from the transformation

$$\begin{Bmatrix} s(0) \\ \lambda(0) \end{Bmatrix} = \Theta^{-1} \begin{Bmatrix} \Sigma(0) \\ \Lambda(0) \end{Bmatrix} \tag{41}$$

where Σ is the physical space state and Λ is the physical space costate.‡ The optimal control solution is then numerically integrated in modal space.

B. Boundary Conditions

The boundary conditions for the free final angle problem are given by:

$$\zeta_0=[\theta(t_0)\eta^T(t_0)]^T \qquad \dot{\zeta}_0=[\dot{\theta}(t_0)\dot{\eta}^T(t_0)]^T \tag{42}$$

$$\eta_f=\eta(t_f) \qquad \dot{\zeta}_f=[\dot{\theta}(t_f)\dot{\eta}^T(t_f)]^T \tag{43}$$

and

$$\theta(t_f)=\text{free} \tag{44}$$

where we impose the constraints that $\eta(t_f)=\dot{\eta}(t_f)=0$ in Eq. (43).

Because the final angle is free, the transversality condition providing the natural boundary condition for the problem follows as:

$$-\Lambda^T(t_f)\delta\Sigma(t_f)=0 \tag{45}$$

where $\delta\Sigma$ is the variation of the physical space state. Since θ_f is free and $\dot{\theta}_f$, η_f, and $\dot{\eta}_f$, are specified, $\delta\Sigma(t_f)$ in Eq. (45) can be written as

$$\delta\Sigma(t_f)=[\delta\theta(t_f)\delta\eta^T(t_f)\delta\dot{\theta}(t_f)\delta\dot{\eta}^T(t_f)]^T$$

$$=[\delta\theta(t_f)0^T\ 0\ 0^T]^T \tag{46}$$

where

$$\delta\theta(t_f)=\delta\Sigma_{11}(t_f)$$

Substituting Eq. (46) into Eq. (45), one obtains

$$\Lambda_{11}(t_f)\delta\Sigma_{11}(t_f)=0 \tag{47}$$

Since $\delta\Sigma_{11}(t_f)$ is arbitrary, it follows that

$$\Lambda_{11}(t_f)=0 \tag{48}$$

Thus, $\theta(t_0)$, $\eta(t_0)$, $\dot{\theta}(t_0)$,$\dot{\eta}(t_0)$, $\Lambda_{11}(t_f)$, $\eta(t_f)$, $\dot{\theta}(t_f)$, and $\dot{\eta}(t_f)$ provide the $4N$, boundary conditions necessary for specifying the physical space optimal control problem for fixed-time free final angle maneuvers.

C. Solution for the Initial Costates for the Free Final Angle Maneuver Problem

The solution for the free final angle optimal control problem can be cast in the form

$$\chi(t)=\Phi(t,t_0)\chi(t_0) \tag{49}$$

where $\Phi(t,t_0)$ is the physical space state transition matrix defined in Eq. (40) and $\chi(t)$ is the merged state vector.

$$\chi(t)=[\Sigma^T(t)\quad\Lambda^T(t)]^T \tag{50}$$

Before the complete optimal control solution can be obtained in Eq. (49), the unknown initial conditions for $\Lambda(t_0)$ must be determined. The linear equation defining the solution for $\Lambda(t_0)$ follows on carrying out the partitioned matrix multiplication for $\Sigma_{12}(t_f)$, ..., $\Sigma_{1N}(t_f)$, $\Sigma_{21}(t_f)$, ..., $\Sigma_{2N}(t_f)$ and $\Lambda_{11}(t_f)$ in Eq. (49) for $t=t_f$, leading to

$$[A]a=b-[B]c \tag{51}$$

where

$$[A]=\begin{bmatrix} \Phi_{\Sigma_{12}\Lambda_{11}} & \cdots & \Phi_{\Sigma_{12}\Lambda_{2N}} \\ \vdots & & \vdots \\ \Phi_{\Sigma_{2N}\Lambda_{11}} & \cdots & \Phi_{\Sigma_{2N}\Lambda_{2N}} \\ \Phi_{\Lambda_{11}\Lambda_{11}} & \cdots & \Phi_{\Lambda_{11}\Lambda_{2N}} \end{bmatrix}$$

$$[B]=\begin{bmatrix} \Phi_{\Sigma_{12}\Sigma_{11}} & \cdots & \Phi_{\Sigma_{12}\Sigma_{2N}} \\ \vdots & & \vdots \\ \Phi_{\Sigma_{2N}\Sigma_{11}} & \cdots & \Phi_{\Sigma_{2N}\Sigma_{2N}} \\ \Phi_{\Lambda_{11}\Sigma_{11}} & \cdots & \Phi_{\Lambda_{11}\Sigma_{2N}} \end{bmatrix}$$

$$a=[\Lambda_{11}(t_0)\ldots\Lambda_{2N}(t_0)]^T \qquad (2N\times 1)$$

$$b=[\Sigma_{12}(t_f)\ldots\Sigma_{2N}(t_f)\Lambda_{11}(t_f)]^T \qquad (2N\times 1)$$

$$c=[\Sigma_{11}(t_0)\ldots\Sigma_{2N}(t_0)]^T \qquad (2N\times 1)$$

Upon solving Eq. (51) for a, using a linear equation solver, the unknown physical space initial costate Λ is found, and the modal space initial conditions are provided by Eq. (41).

VIII. Applications to Example Maneuvers

Several example maneuvers have been determined using the above formulations. For all cases, the geometry of Fig. 1 has been assumed with the following configuration parameters: the inertia of the undeformed structure $\hat{I}$ is 6764 kg-m^2; the mass per unit length of the four identical elastic appendages, ρ, is 0.04096 kg/m; the length of each cantilevered appendage, L, is 35 m; the flexural rigidity of the cantilevered appendages, EI, is 1500 kg-m^3/s^2; and the radius of the rigid

‡$\Sigma=[\zeta^T\dot{\zeta}^T]^T=[\Sigma_1^T\Sigma_2^T]^T$, $\Sigma_1=\zeta=[\Sigma_{11}\Sigma_{12}\ldots\Sigma_{1N}]^T$,

$\Sigma_2=\dot{\zeta}=[\Sigma_{21}\Sigma_{22}\ldots\Sigma_{2N}]^T$, $N=n+1$

$\Lambda=[\Lambda_1^T\Lambda_2^T]^T$, $\Lambda_1=[\Lambda_{11}\Lambda_{12}\ldots\Lambda_{1N}]^T$, $\Lambda_2=[\Lambda_{21}\Lambda_{22}\ldots\Lambda_{2N}]^T$

hub, r, is 1 m. In the integrations over the mass stiffness distributions, the radius of the hub is not neglected.

In Eq. (5) the following comparison functions

$$\phi_p(x-r) = 1 - \cos\left[\frac{p\pi(x-r)}{L}\right] + \frac{1}{2}(-1)^{p+1}\left[\frac{p\pi(x-r)}{L}\right]^2 \qquad (p=1,2,\ldots,\infty) \qquad (52)$$

which satisfy the geometric and physical boundary conditions

$$\phi_p\Big|_{x=r} = \phi_p'\Big|_{x=r} = \phi_p''\Big|_{x=r+L} = \phi_p'''\Big|_{x=r+L} = 0 \qquad (53)$$

of a clamped-free appendage have been adopted as assumed modes.

With reference to Table 1 and Figs. 4-10, the graphical summaries of the state and control time histories are discussed qualitatively.

Case 1 (Fig. 4) is a rest-to-rest maneuver with only one controller on the rigid hub. Case 2 (Fig. 5) is an identical maneuver with one additional controller on each appendage. Comparing the two cases, one finds that the addition of appendage controllers reduces the peak amplitude of the first and second modes, while increasing the third mode peak amplitude. The peak torque is also slightly reduced.

Case 3 (Fig. 6) is a spin acceleration maneuver which requires the vehicle's angular velocity to increase. If the final angle is permitted to go free, the overall system response can be improved as measured by peak flexural deformations and peak torque requirements.

Case 4 (Fig. 7) is the nonlinear version of case 3. The first mode participation decreases while the higher modes are excited somewhat more. In addition, the peak hub control torque increases. Notice that the modal amplitude time histories for case 4 have seven major dips while for case 3 there are six dips. For cases where the initial and final angular velocities are lower than in cases 3 and 4, it is found that the difference between linear and nonlinear runs is small.

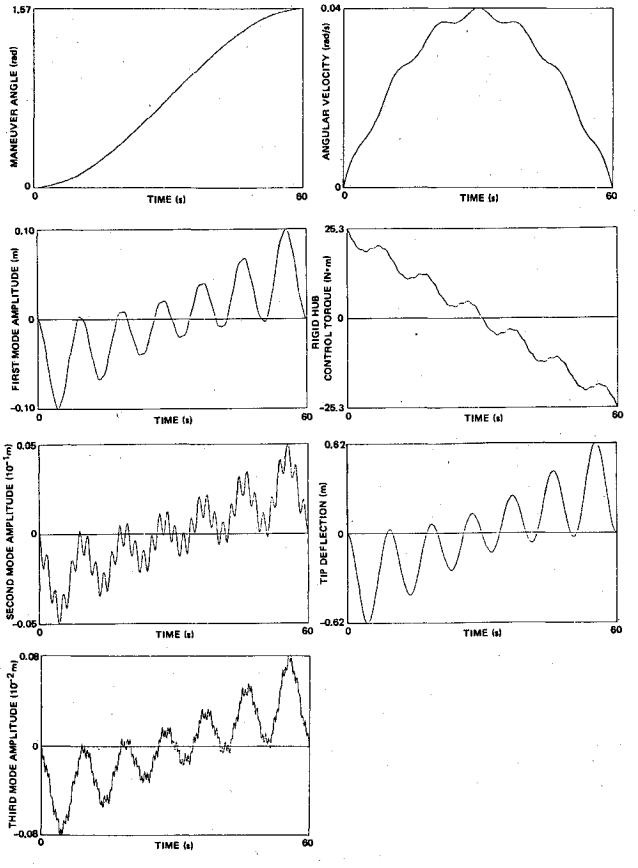

Fig. 4 Case 1, rest-to-rest maneuver, 1 control.

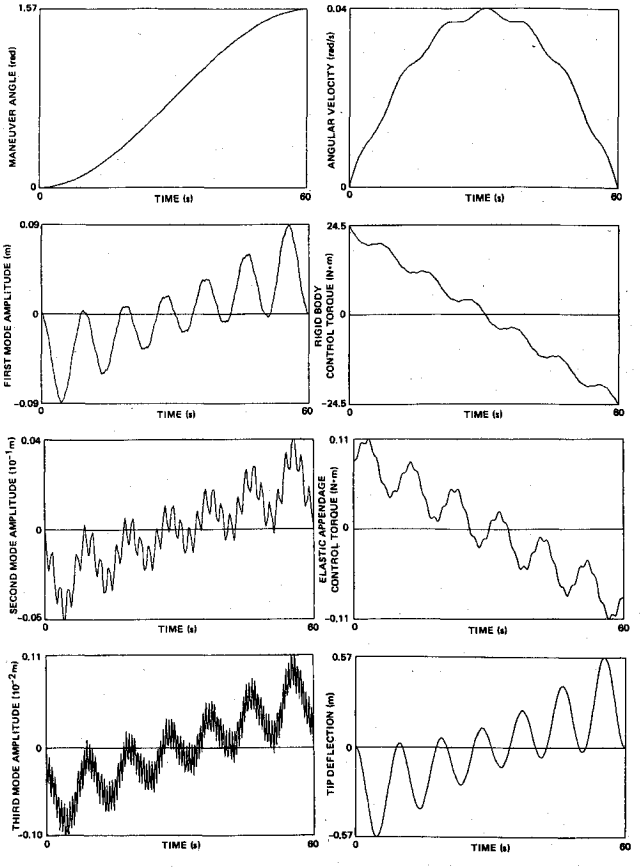

Fig. 5 Case 2, rest-to-rest maneuver, 5 controls.

Table 1 Description of test case maneuvers

Case no.	$t_f - t_0$	No. of modes n	θ_0, rad	$\dot{\theta}_0$, rad/s	θ_f, rad	$\dot{\theta}_f$, rad/s	No. of controls	W_{uu}^a	W_{ss}^b
1	60 s	3	0	0	$\pi/2$	0	1	1	$[I]^*$
2	60 s	3	0	0	$\pi/2$	0	5	$[I]^\circ$	$10^{-3}[I]^*$
3	60 s	3	0	0.5	33.5	0.6	5	$[I]^\circ$	$10^{-3}[I]^*$
4[c]	60 s	3	0	0.5	33.5	0.6	5	$[I]^\circ$	$10^{-3}[I]^*$
5	60 s	3	0	0.5	–	0.6	5	$[I]^\circ$	$10^{-3}[I]^*$
6	5 s	10	0	0	0.2	0	5	$[I]^\circ$	$10^{-3}[I]^*$

[a] $[I]^\circ$ is an identity matrix with the first element set to 10^{-3}, setting a lower weight on the rigid body torque.
[b] All the W_{ss} matrices are set to diagonal matrices in physical space, and then mapped into modal space, via the Equation $W_{ss} = E^T W_{ii} E$ for $i=1,2$. $[I]^*$ is an identity matrix with the first element set to 10^{-2}. This sets a lower weight on the maneuver angle.
[c] Case 4 simulates the example structure with nonlinear kinematics.

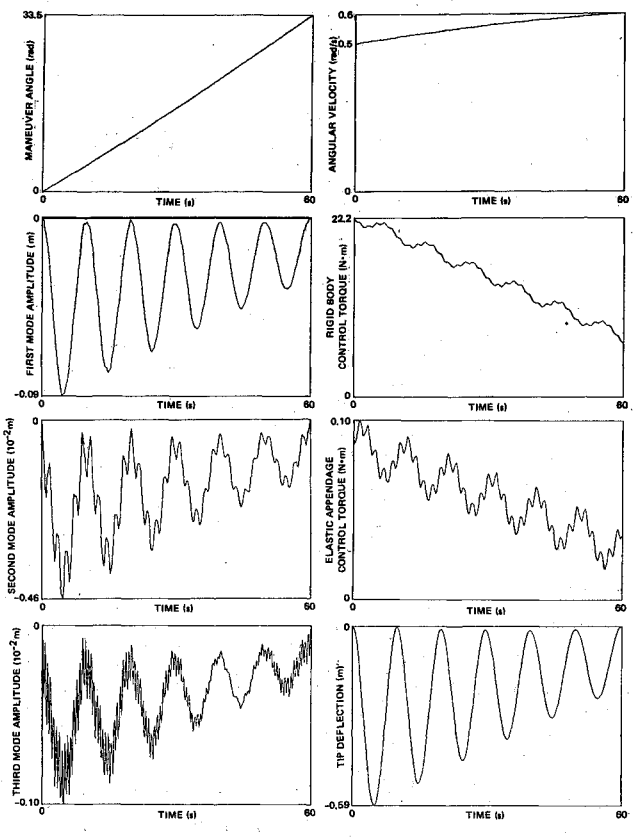

Fig. 6 Case 3, spin acceleration maneuver, 5 controls.

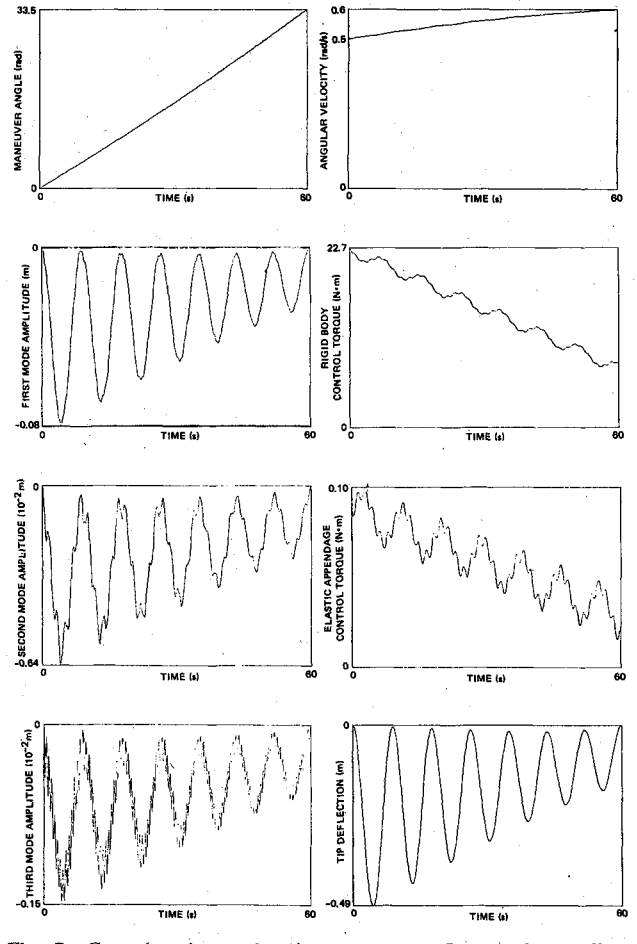

Fig. 7 Case 4, spin acceleration maneuver, 5 controls, nonlinear kinematics.

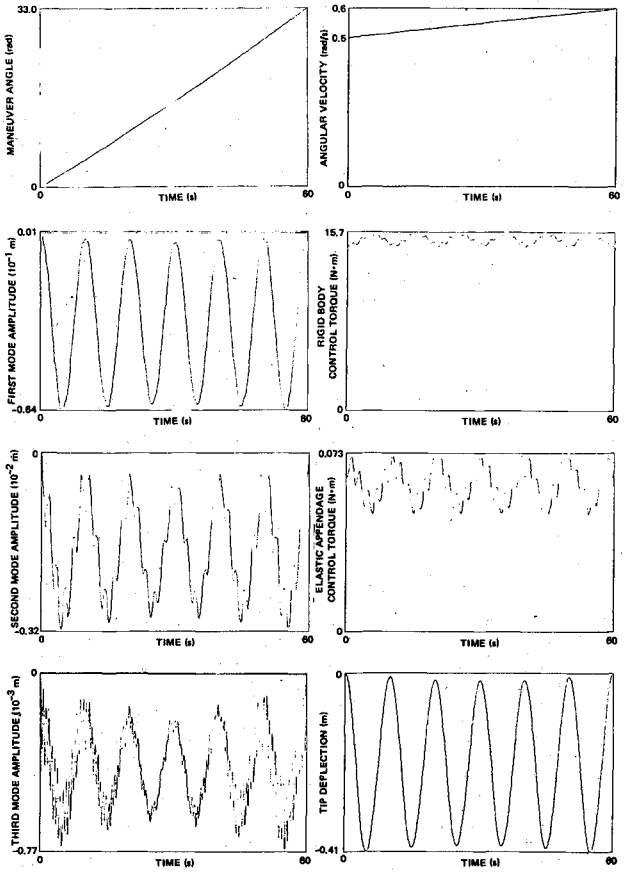

Fig. 8 Case 5, spin acceleration maneuver, free final angle, 5 controls, linear kinematics.

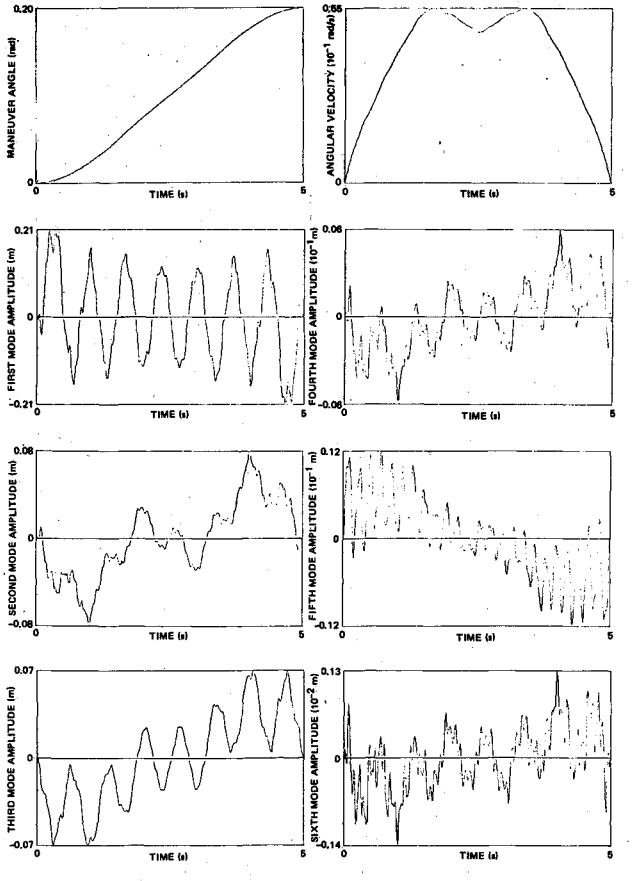

Fig. 9 Case 6, rest-to-rest maneuver, 10 modes, 5 controls.

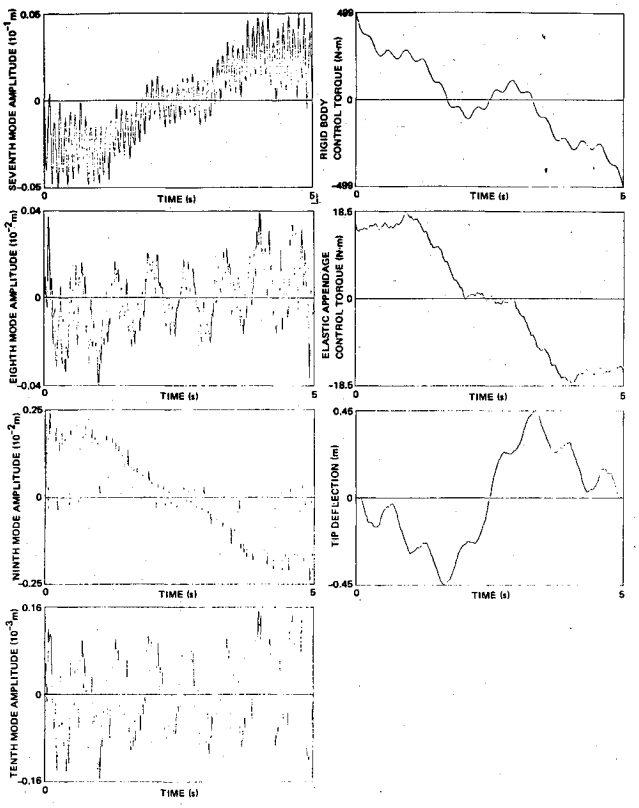

Fig. 10 Case 6, continued.

Case 5 (Fig. 8) is a spin acceleration maneuver where the final maneuver angle is free. The final angle of 33.0 rad is determined by the optimal control problem. By running several simulations with specified final angles less than and greater than 33.0 rad, and on comparing the corresponding performance indices, one finds that the performance index is indeed minimum when the final angle is 33.0 rad, as selected by the control algorithm.

Case 6 (Figs. 9 and 10) represents a simple linear rest-to-rest maneuver where ten elastic modes of the structure are controlled. It is of interest to note that the terminal boundary conditions for θ_f, $\dot{\theta}_f$, $\eta_f = 0$, and $\dot{\eta}_f = 0$ were achieved with an error no larger than 1×10^{-11}.

In general, a change in the magnitude of the state weight matrix W_{ss} has little or no effect on the torque histories for the single controller cases. However, when control torques are applied to the appendages, a change in the magnitude of the W_{uu} matrix can significantly affect the appendage torque and modal amplitude time histories.

If required, many additional modes can be run in the simulations. In all example cases run, the linear solution obtained from Eq. (24) has been iteratively refined using Eq. (38) by replacing $\phi_{s\lambda}$ for the nonlinear problem with the $\phi_{s\lambda}$ used in Eq. (24). For more example maneuvers, see Ref. 9.

IX. Concluding Remarks

The results of this paper provide a basis for systematic solution of optimal large-angle single-axis spacecraft rotational maneuvers, when a distributed control system is employed. In addition, a continuation method is presented and an example of a nonlinear two-point boundary-value problem provided which demonstrates the utility of the formulation described herein. Moreover, we have found that unless very high angular rates are achieved during the maneuver, the linear and nonlinear solutions differ very slightly. The formulation for a free final angle maneuver is presented for the case in which only the angular rate is of interest.

References

[1] Junkins, J.L. and Turner, J.D., "Optimal Continuous Torque Attitude Maneuvers," Paper 78-1400, *AIAA/AAS Astrodynamics Conference,* Palo Alto, Calif., Aug. 1978.

[2] Swigert, C.J., "Shaped Torque Technique," Paper 78-1692, *AIAA Conference on Large Space Platforms Future Needs and Capabilities,* Los Angeles, Calif., Sept. 27-29, 1978.

[3] Markley, F.L., "Large Angle Maneuver Strategy for Flexible Spacecraft," Paper 79-156, *AAS/AIAA Astrodynamics Specialist Conference,* Provincetown, Mass., June 25-27, 1979.

[4] Breakwell, J.A., "Optimal Feedback Maneuvering of a Flexible Spacecraft," AAS Preprint 79-157, *AAS/AIAA Astrodynamics Conference,* June 1979.

[5] Alfriend, K.T., Bercaw, R.W., and Longman, W.S., "On Frequency Response Interpretations of Optimal Slewing Maneuvers," *Proceedings of the Second VPI&SU/AIAA Symposium on Dynamics and Control of Large Flexible Spacecraft,* Blacksburg, Va., June 21-23, 1979.

[6] Turner, J.D. and Junkins, J.L., "Optimal Large-Angle Single-Axis Rotational Maneuvers of Flexible Spacecraft," *Journal of Guidance and Control,* Vol. 3, Nov.-Dec. 1980, pp. 578-585.

[7] Meirovitch, L., *Methods of Analytical Dynamics,* McGraw-Hill, New York, 1970, p. 68.

[8] Meirovitch, L., "A Stationary Principle for the Eigenvalue Problem for Rotating Structures," *AIAA Journal,* Vol. 14, Oct. 1976, pp. 1387-1394.

[9] Chun, H.M., "Optimal Distributed Control of a Flexible Spacecraft During a Large-Angle Rotational Maneuver," Master's Thesis, Massachusetts Institute of Technology, Cambridge, Mass., 1982.

[10] Moler, C. and Loan, C.V., "Nineteen Dubious Ways to Compute the Exponential of a Matrix," *SIAM Review,* Vol. 20, No. 4, Oct. 1978, pp. 801-836.

[11] Ward, R.C., "Numerical Computation of the Matrix Exponential with Accuracy Estimate," *SIAM Journal of Numerical Analysis,* Vol. 14, No. 4, Sept. 1977, pp. 600-610.

[12] Schmidt, W.F., "Adaptive Step Size Selection for Use with the Continuation Method," *International Journal for Numerical Methods in Engineering,* Vol. 12, 1978, pp. 677-694.

[13] Deuflhard, P., Pesch, H.J., and Rentrap, P., "A Modified Continuation Method for the Numerical Solution of Nonlinear Two-Point Boundary-Value Problems by Shooting Techniques," *Numer. Math.,* Vol. 26, 1976, pp. 327-343.

[14] Dennis, J.E. Jr. and Schnabel, R.B., "Lease Change Secant Updates for Quasi-Newton Methods," *SIAM Review,* Vol. 21, No. 4, Oct. 1979, pp. 443-459.

[15] Greenstadt, J., "Variations on Variable-Metric Methods," *Mathematics of Computation,* Vol. 24, No. 109, Jan. 1970, pp. 1-22.

[16] Goldfarb, D., "A Family of Variable-Metric Methods Derived by Variational Means," *Mathematics of Computation,* Vol. 24, No. 109, Jan. 1970, pp. 23-26.